

Determination of hydrogen diffusivity depending on the hydride concentration in titanium-hydride by means of the diffraction-enhanced X-ray imaging method

Kaoru Mizuno, Takashi Kanai*, Kei-ichi Hirano** and Hiroyuki Okamoto***

Interdisciplinary Faculty of Science and Engineering, Shimane University, Matsue 690-8504, Japan

FAX: 81-852-32-6409, e-mail: mizuno@riko.shimane-u.ac.jp

* Faculty of Science, Kanazawa University, Kanazawa 920-1192, Japan

FAX: 81-76-234-4360, e-mail: kanai0904@gmail.com

** High Energy Accelerator Research Organization, Tsukuba 305-0801, Japan

FAX: 81-29-864-2801, e-mail: keiichi.hirano@kek.jp

*** School of Medicine, Kanazawa University, Kanazawa 920-0942, Japan

FAX: 81-76-234-4360, e-mail: okamoto@mhs.mp.kanazawa-u.ac.jp

The X-ray refraction imaging technique was applied to the quantitative study of hydrogen diffusion in titanium-hydride. Hydrogen diffusivity in titanium-hydride was determined by direct observation of the hydride. The hydride was formed on the surface of titanium by electrolytic-charging at 63°C. The specimens were cut into 1-mm thick slices for cross-sectional observations. The hydride layer was observed using the diffraction-enhanced X-ray imaging (DEI) method with asymmetric analyzer. Boundaries between titanium and the hydride were observed as thick black or white lines parallel to the specimen surface in the DEI images similar to previously reported results. Hydride distribution caused by hydrogen diffusion from the surface was converted to the intensity profiles of refraction images of the hydride using the measured rocking curve from an analyzer. The hydrogen diffusivity was calculated from the intensity profiles using the solution of the appropriate diffusion equation. The obtained hydrogen diffusivity in titanium-hydride depended upon the hydrogen concentration. The diffusivity showed good agreement with the widely accepted values in the low hydride concentration region.

Key words: hydrogen, titanium-hydride, diffraction-enhanced X-ray imaging

1. INTRODUCTION

Considerable effort has been expended towards investigating the interactions between hydrogen and metals for various applications, such as the development of hydrogen-storage materials for example. Consequently, significant knowledge has been acquired in this area. In titanium containing higher concentrations of hydrogen, titanium atoms span a slightly tetragonally distorted face centered tetragonal lattice and hydrogen atoms occupy tetrahedral interstitial sites [1, 2]. In a study on the diffusion of hydrogen in titanium and hydride, Wipf et al. [3] determined the diffusion coefficient value of hydrogen in titanium-hydride, and have reported the activation energy of diffusion to be 0.49 eV. However, these investigations dealt with less common or indirect detection techniques such as NMR and mechanical spectroscopy (vibrating reed technique). It is necessary to establish a direct observation technique for hydrogen or hydrides in metals for investigation of the metal-hydride system.

Imaging techniques utilizing high-energy X-rays, such as projection radiography and tomography, have been used for many years to non-destructively observe the image contrast of internal structures of objects. In conventional imaging techniques utilizing high-energy X-rays, the X-rays that pass through an object along different paths are absorbed differently, and hence, the intensity pattern of the emerging beam records the distribution of absorbing materials within the specimen. In general, the difference between the absorption coefficient of a metal and its hydride is negligibly small. Therefore, it is impossible to visualize the hydride in the matrix metal. However, there is another X-ray imaging technique called phase contrast imaging or refraction contrast imaging [4-7]. This approach offers improved contrast sensitivity, especially when imaging weakly absorbing specimens. The refraction contrast X-ray imaging technique has been successfully used previously, and is seeing excellent and rapid progress as a diagnostic tool in medicine, biology and materials science, because of

the application of highly parallel X-ray beams from synchrotron radiation sources [8-10]. Although the difference in the real part of refraction indexes between titanium and titanium-hydride is extremely small, about 10^{-8} for 30 keV X-rays, we were able to visualize a high-contrast projection image of the hydride using refraction contrast radiography [11]. The most suitable refraction radiography technique for metal physics is the diffraction-enhanced X-ray imaging method (analyzer-based X-ray phase contrast imaging) because it is easy to separate the refraction images and absorption images in an X-ray photograph obtained by this imaging method. As mentioned above, these techniques have been widely used, however, almost all investigations were limited to qualitative observations. A few quantitative studies, such as determination of the activation energies of physical phenomena, have been reported [12]. In this investigation, observations were limited for specimens with thick hydride layer ($>100\mu\text{m}$) because of its low-resolution power. Therefore, we applied the X-ray DEI method with asymmetrical reflection analyzer for magnification of layer images of hydride and determined the diffusivity of hydrogen diffusion in titanium-hydrides formed by electrolytic-charge with different charging time on α -titanium surface.

2. EXPERIMENTAL PROCEDURES

Polycrystals of α -titanium (99.99 at. %) supplied by Sumitomo Titanium Co. Ltd were used for specimens in the present investigation. The specimen's dimensions were approximately $1.0 \times 5 \times 15 \text{ mm}^3$. The specimens were annealed at 800°C for 1 hour under ultrahigh vacuum before hydrogen charging. To observe a cross section of specimens, we prepared specimens with hydride deposited on the surface by an electrolytic-charge. The charge was carried out in 1-N sulfuric acid at 63°C . Electrolytic-charging times and current density were 10, 22 and 48 hours and 5 mA/mm^2 , respectively.

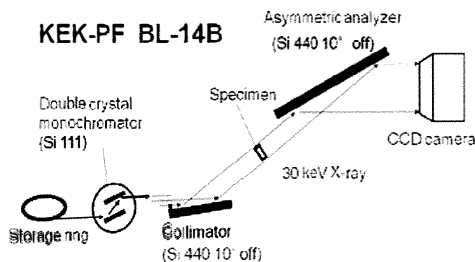


Fig. 1 Schematic diagram of the beam line and experimental setup for diffraction-enhanced X-ray imaging method.

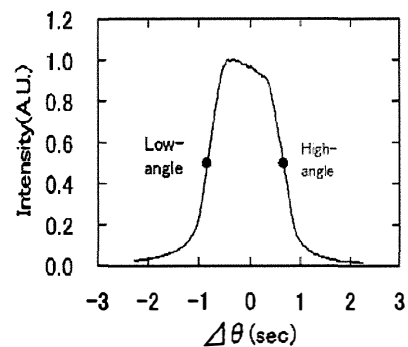


Fig. 2 Measured rocking curve of the analyzer for the transmitted X-rays from the specimen. We recorded the diffracted X-rays from the analyzer on CCD camera at each offset angle of $\Delta\theta$ shown as closed circles.

The specimen was cut into a 1-mm thick slice for cross-sectional observation.

The present observations were performed at a vertical-wiggler beam line, BL-14B (precision X-ray optical station), at the Photon Factory in the High Energy Accelerator Research Organization (KEK) in Tsukuba, Japan. A schematic experimental setup for X-ray diffraction-enhanced imaging method is shown in Fig. 1. The X-ray energy was tuned to 30 keV by the beam line monochromator. The collimator and the analyzer were cut from a silicon ingot, and their surfaces were mechano-chemically polished to remove defects and strains. The collimator was adjusted at the asymmetric 440-diffraction condition. The angle between the crystal surface and the reflecting plane was 10° . The analyzer was adjusted close to the asymmetric 440-diffraction condition. The angle between the crystal surface and the reflecting plane for asymmetric reflection was 10° (asymmetric ratio: 0.112). Horizontal magnification of the image by the asymmetric reflection was 9 times. The distance between specimen and film was about 0.5 m. The exposure time of CCD-camera was about 20 s.

3. EXPERIMENTAL RESULTS AND DISCUSSION

The rocking curve of the asymmetric reflection analyzer for the transmitted X-rays from the specimen was measured and is shown in Fig.2. We recorded the diffracted X-rays from the analyzer on a CCD-camera at each offset angle of $\Delta\theta$ from the Bragg condition shown as closed circles in Fig.2. These two photographs show low-angle ($\Delta\theta = -0.80''$) and high-angle ($\Delta\theta = 0.65''$) side images of the rocking curve. Figure 3 shows diffraction-

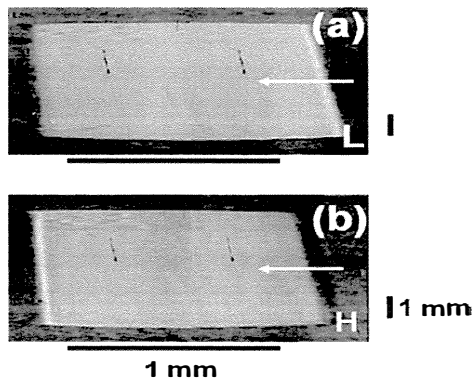


Fig. 3 Diffraction-enhanced images of the cross-section of the specimens taken by 30 keV X-ray. The images are taken using the asymmetric reflection analyzer for magnification of layer images of hydride. The marks L and H show low-angle and high-angle side images of the rocking curve, respectively.

enhanced images of the cross-section of titanium-hydride specimens using the asymmetric reflection. The low- and high-angle images are shown in Fig. 3 (a) and 3 (b), respectively. Electrolytic-charging time of the specimen was 22 hours. There is hydride observed in Fig.3. The circumference of the specimen shows white and black contrast images and the image is reversed between Fig. 3 (a) and 3 (b) similar to previously reported results [10]. Because hydrogen charging of this specimen was carried out at 63 °C, hydrogen atoms could not diffuse into the crystal so fast on account of the high migration energy of hydrogen (0.49 eV) [3]. Thus, hydrides were formed on the near surface of the specimen. Figure 4 shows intensity distribution along the white thin arrow from the surface of 22 h charged specimens shown in Fig. 3 (a) and (b). The square and circle in Fig. 4 indicate intensity of low-angle side image, Fig. 3 (a), and high-angle side one, Fig. 3 (b), respectively. However, these intensity profiles contain absorption effect by the specimen. In order to exclude absorption, we introduce the net X-ray intensity of refracted beam, ΔI ,

$$\Delta I = I_H - I_L, \quad (1)$$

where I_H and I_L are intensity of high-angle image and low-angle image shown in Fig. 4, respectively. Intensity profile, ΔI , of 22 h charged specimens is shown in Fig. 4 as triangles.

In order to determine the distribution of hydride in titanium, we obtained the deviation angle of X-ray by refraction from intensity profile, ΔI , using

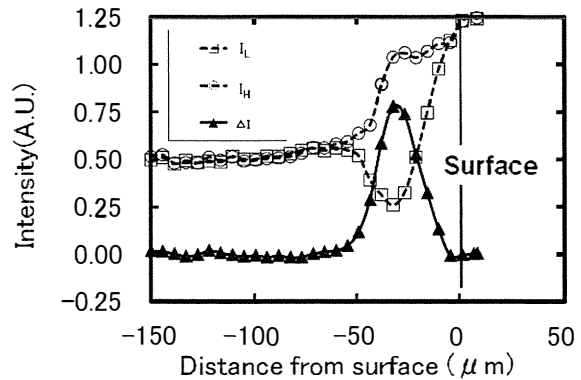


Fig. 4 Intensity distribution of Fig. 3(a) and 3(b) toward inside from the surface.

The squares and circles indicate intensity of low-angle side image, Fig. 3 (a), and high-angle side one, Fig. 3 (b), respectively. The triangles indicate the net intensity profiles of refracted X-ray beam of specimen.

the rocking curve shown in Fig. 2. Next, the distribution of refraction index was calculated from the deviation angle of X-ray using Snell's law. Finally distribution of ratio of hydride and titanium, the concentration profile of hydride, was obtained from that of the refraction index. The real part of refraction index of hydride and titanium for 30 keV X-ray is $1-1.01 \times 10^{-6}$ and $1-0.97 \times 10^{-6}$, respectively [13].

The obtained concentration profile of hydride of 10, 22 and 48 h charged specimens was shown in Fig.5. In the titanium-hydrogen system, heat solution of hydrogen into titanium and formation energy of hydride, TiH_2 , are both negative [14]. Hydrogen atoms in the titanium immediately formed hydride. So we can consider the concentration profile of hydride as distribution of hydrogen as shown in

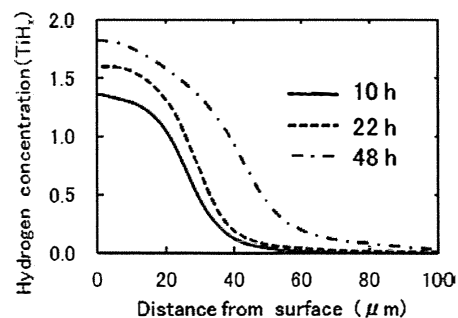


Fig. 5 The hydrogen concentration vs. distance from the specimen surface. High concentration region of hydrogen was moved toward the inner area of the specimen in proportion as the charging time.

Fig.5. Figure 5 shows the hydrogen concentration vs. distance from the specimen surface. High concentration region of hydrogen was moved toward the inner area of the specimen in proportion as the charging time. The concentration profile of hydrogen in titanium was determined to accuracy of the order of micrometer by means of the asymmetric reflection analyzer. In spite of convenient means, the obtained results of hydrogen concentration from the present method showed the improvement of spatial resolution.

Concentration profile of hydrogen in Fig. 5 shows complicated shape rather than that obtained by symmetric analyzer [15]. The profile curves in Fig.5 were not able to simulate using a solution of the one-dimensional diffusion equation with constant diffusion coefficient. Therefore, we try to evaluate the diffusivity of hydrogen depending on the hydrogen concentration from the results.

The surface concentration of hydrogen was maintained constant during the electrolytic charging in the present experiment. Then, the diffusion coefficient of hydrogen depending upon the hydrogen concentration $D(c)$ is expressed by Shewmon as follows [16].

$$D(c) = - \frac{\sum_x \left(\frac{\partial c(x,t)}{\partial t} \right)_x \Delta x}{\left(\frac{\partial c(x,t)}{\partial x} \right)_t} \quad (2)$$

where c is the concentration of hydrogen, t is the charging time, x is the space coordinate measured normal to the specimen surface. In this equation,

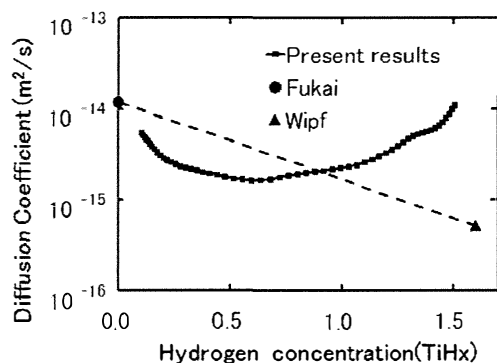


Fig.6 Diffusion coefficients of hydrogen in titanium-hydride for different hydrogen concentration. Dotted line shows the interpolation between hydrogen diffusivity in pure titanium reported by Fukai and in $\text{TiH}_{1.6}$ reported by Wipf.

numerators and dominator are corresponding to the displacement in longitudinal and horizontal axis in the figure 4, respectively. The calculated hydrogen diffusion coefficient depending upon the hydrogen concentration is plotted in Fig. 6. The hydrogen diffusivity in Fig.6 clearly shows concentration dependence of hydrogen in the hydride. The coefficients in pure Ti and $\text{TiH}_{1.6}$ are only reported as shown in Fig. 6 [14,3]. In the low hydride concentration ($x < 0.6$), present results in Fig.6 showed good agreement with the interpolation of previously reported values. However, there is a discrepancy between the present results and the interpolation line in the high concentration region. Diffusion mechanism of hydrogen in the high hydride region will be varying according to hydride concentration. In nickel, generation of great deal of vacancy reported under high temperature and high hydrogen pressure or during electro-crystallization [17]. It is possible to form a large amount of vacancy in Ti during an electrolytic-charging.

4. SUMMARY

We determined the hydrogen diffusivity depending upon the hydrogen concentration in titanium-hydride by the direct observation of hydride using diffraction-enhanced X-ray imaging method. And the values showed good agreement with previously reported ones in the low hydride concentration region.

5. ACKNOWLEDGMENTS

This work has been performed under the approval of the Photon Factory Advisory Committee (Proposal No. 2010G622). We also thank Sumitomo Titanium Co. Ltd for supplying high purity titanium crystals.

5. REFERENCES

- [1] L. D. Bustard and R. M. Cotts: Phys. Rev. B **22** 12-17 (1980).
- [2] E. Zuzek, J. P. Abriata, A. San-Martin, F. D. Manchester: Bull. Alloy Phase Diagr. **11** 385-391 (1990).
- [3] H. Wipf, B. Kappesser and R. Werner: J. Alloys and Compounds **310** 190-197 (2000).
- [4] K. Aoyagi, E. P. Torres, T. Suda, S. Ohnuki: J. Nuclear Materials **283-287** 876 (2000).
- [5] V. A. Somenkov, A. K. Tkach and S. Sh. Shil'shtein: Sov. Phys. Tech. Phys. **36** 1309 (1991).
- [6] J. Kirz: Q. Rev. Biophys., **28** 33-39 (1995).

- [7] A. Snigirev, I. Snigreva, V. Kohn, S. Kuzunetsov and I. Schelokov: *Rev. Sci. Instrum.* **66** 5486-5490 (1995).
- [8] D. Chapman, W. Thomlinson, R. E. Johnston, D. Washburn, E. Pisano, N. Gmuer, Z. Zhong, R. Menk, F. Arfelli and D. Sayers, *Phys. Med. Biol.* **42** 2015 (1997)
- [9] N. Yagi, Y. Suzuki, K. Umetani, Y. Kohmura and K. Yamasaki: *Med. Phys.* **26** 2190-2195 (1999).
- [10] K. Kagoshima, Y. Tsusaka, K. Yokoyama, K. Takai, S. Takeda and J. Matsui: *Jpn. J. Appl. Phys.* **38** L470-L474 (1999).
- [11] K. Mizuno, T. Kobayashi, F. Fujiki, H. Okamoto, Y. Furuya, K. Hirano: *J. Alloys and Compounds* **402** 109-115 (2005).
- [12] K. Mizuno, Y. Furuya, K. Hirano and H. Okamoto: *Physics Status Solidi (a)* **204** 2734-2739 (2007).
- [13] <http://www-cxro.lbl.gov>
- [14] Y. Fukai: *The Metal-Hydrogen System* (Springer Verlag, New York, 1993), Chap.1, p. 38.
- [15] K. Mizuno, Y. Furuya, K. Hirano and H. Okamoto: *Trans. Mater. Res. Soc. Jpn.* **34** 229-232 (2009).
- [16] P. G. Shewmon: *Diffusion in Solid* (MacGraw-Hill, New York, 1963)
- [17] Y. Fukai: *J. Alloys and Compounds* **365-357** 263-269 (2003).

(Received December 27, 2011; Accepted May 26, 2012)

